

Impedance control design for on-orbit docking using an analytical and experimental approach*

Zisos Mitros, Georgios Rekleitis, *Member, IEEE*, Ilias Patsiaouras,
and Evangelos Papadopoulos, *Senior Member, IEEE*

Abstract— An important phase in On-Orbit servicing missions is robotic docking. Successful docking is subject to a number of parameters and conditions. In this work, the robotic impact docking between two space systems is considered. The docking of a robotic Chaser to a Target spacecraft is modeled using a multibody approach. The impedance properties required for an impedance controller that will ensure adequate probe-drogue contact time for docking are computed and are related with their mechanical counterparts. This time is derived analytically employing a mechanical equivalent system, and validated experimentally on a planar zero gravity emulator facility, allowing the selection of impedance parameters for successful docking.

I. INTRODUCTION

The exploitation and commercialization of space will require in the near future robotic systems capable of construction and assembly of large infrastructure, as well as of tasks such as astronaut assistance, docking and berthing for servicing missions, or space debris handling. The above fall under the broad term of On-Orbit Servicing (OOS). A number of space agencies have addressed OOS activities with missions such as JAXA's ETS-VII [1], NASA's Orbital Express [2] and the Robotic Refueling Mission (RRM) [3], or with on-going projects, such as ESA's hArmonised System Study on Interfaces and Standardization of fuel Transfer (ASSIST) [4]. Autonomous robotic OOS can vastly improve on-orbit operations, and in parallel, reduce the risks to human life.

Docking, i.e. the firm connection between two spacecrafts, or between a free-flying robotic servicer and a serviced spacecraft, is important in many OOS tasks. It is a demanding task due to impacts, lack of fixed base, and dynamic coupling [5], requiring intense astronaut training. Therefore, it is a clear candidate for autonomous execution; to this end, extensive studies and experiments are needed.

A common docking scheme, which is also adopted in this paper requires that the end-effector enters a drogue and stays there for finite time during which a mechanism is deployed to connect the two spacecrafts (soft docking) see Figure 1. If this time is not enough, then docking fails or the mechanism jams. Therefore, understanding the dynamics and control of the process is of critical importance. Being able to estimate contact time and velocities based on spacecraft parameters, controller gains, and relative motions prior to impact, is of vital importance for successful docking.

* Partial support by the ESA/GMV ASSIST, and the FP7-SME-2013/605420 HexaTerra projects is acknowledged.

Z. Mitros (zmitros@gmail.com), G. Rekleitis (georek@gmail.com), Ilias Patsiaouras (ilias.patsiaouras@gmail.com), and E. Papadopoulos (egpapado@central.ntua.gr, +30-210-772-1440) are with the School of Mechanical Engineering, National Technical University of Athens, 15780 Athens, Greece.

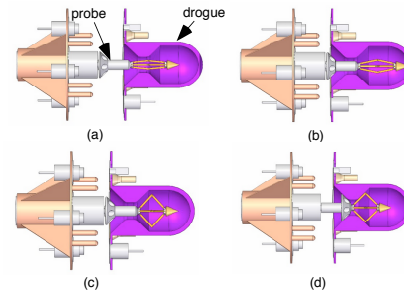


Figure 1. Chaser (not shown) probe and Target (not shown) drogue during docking. (a) Probe entering the drogue. (b) Impact, (c) Soft docking allowing relative motions, (d) Hard (rigidized) docking, [4].

Recent works on docking take into account the system dynamics, either post, [6], or prior to impact, [7].

During docking, hard collisions may result in serious damage or destruction of a target and failure of the mission, as a result, compliance plays an important role to the success of the mission. Two approaches are often used, passive and active compliance. Passive compliance utilizes mechanical compliance with no control time delay but with limitation for operations. On the other hand, active compliance is a big research topic in robotics which can bring solutions to many problems. Impedance Control (IC) is an example of active compliance control which incorporates the use of lumped parameters [13]. For a single manipulator in dynamic interaction with its environment, IC can regulate the relationship between end-effector position and interaction force, [14]. IC can be used also, to minimize the impact forces and the developed impulses by using the concept of virtual mass [12]. To manipulate an object by multi-arm robotic systems, the *Multiple Impedance Control* (MIC) has been proposed and compared with various control strategies in [15]. The MIC enforces a desired reference impedance on both the manipulator end-points, and the manipulated object, and hence, an accordant motion of the manipulators and payload is achieved. An important part in IC is the proper tuning of impedance parameters. A parameter tuning method by setting a desired coefficient of restitution and a desired damping ratio was proposed in [11].

To model impact docking and validate control methodologies, the employment of alternative modeling approaches is needed [8]. Lumped parameters models are used for rigid impacting bodies providing satisfactory results, [9]. To obtain experimentally results, various concepts have been identified. A Hardware-In-the-Loop (HIL) simulator was used via a method to model the impact between two rigidly fixed systems, [10]. However, the time delay due to HIL set limits to the system parameters that could be used. Furthermore, the contact duration was shorter than the time needed to compute the robot dynamics, adding energy to the

system and leading to instability of the closed-loop system and inconsistencies in the simulation results. Another docking procedure was proposed, in which the systems were rigidly fixed and not floating as they are in space; hence the results obtained involve inaccuracies [11]. Contact dynamics models were validated against experimental results in [16]. However, the employed fixture was rigidly fixed; hence inaccuracies resulted. For these reasons, air bearings facilities present a high fidelity emulation system, if the planar motion of the robots is adequate. The Control Systems Laboratory (CSL) at the National Technical University of Athens (NTUA) has developed a planar air bearing emulator to test most complex operations such as docking and implementation of different kind of control theories [18].

In this paper, docking of a robotic Chaser to a Target spacecraft employing an impedance-controlled manipulator is studied. In order to gain some further insight on the docking process and to derive some useful conclusions, the docking is modeled using a simplified 1D multibody approach, as is common in the literature [5]. The impedance gains required for an impedance controller that will ensure adequate probe-drogue contact time for docking are compared with their mechanical counterparts via the employment of a simple mechanical equivalent system; adequate though to draw some first conclusions. Moreover, the analytically derived conclusions, are also validated experimentally on the CSL planar zero gravity emulator facility, allowing the selection of impedance parameters for successful docking.

II. DOCKING SCENARIO AND REQUIREMENTS

One of the proposed scenarios for docking between two spacecrafts consists of a manipulator mounted on a Chaser and equipped with a probe, entering a drogue, mounted on a Target spacecraft. The probe is required to remain inside the drogue cavity for a finite time t_d , so that the docking mechanism deploys and locks the probe in the drogue cavity, see Figure 1c.

Based on the approach of equivalent two-body system modelling (see also [17]), the controllable Chaser spacecraft, consists of a main body and an articulated manipulator. The main body (base) with its appendages are lumped to a mass m_c while the probe tip having mass m_{pt} . The manipulator is modeled as an impedance-controlled actuator. The Chaser body position is denoted by x_c and the position of the probe tip by x_{pt} , while the Target position is denoted by x_t , see Figure 2. The probe-drogue contact is modelled as a very stiff spring of stiffness k_i and damping b_i , modeling energy losses.

Initially, the Chaser spacecraft moves at a constant relative velocity $u_{rel,0}$ with respect to the Target, approaching the Target spacecraft and its drogue. The motion of the probe-tip inside the drogue cavity consists of three phases: (a) *Entering*, from the moment the probe-tip enters the drogue until it impacts with the far end of the cavity, (b) *Impact* and (c) *Exiting*, from the moment the impact is concluded and the probe-tip loses contact with the drogue cavity far end, until it exits the cavity. Thus, the total time t_{tot} the probe-tip remains inside the drogue cavity, is given by,

$$t_{tot} = t_{en} + t_{imp} + t_{ex} \quad (1)$$

where t_{en} is the entering time, t_{imp} is the impact time and t_{ex} is the exiting time. For the docking mechanism to have enough time to be deployed and lock the probe-tip inside the drogue

cavity, this time must be no less than t_d , i.e.,

$$t_{tot} \geq t_d \quad (2)$$

Clearly, the entering time t_{en} depends on the initial relative velocity $u_{rel,0}$ and on the drogue cavity length d_{dc} only:

$$t_{en} = d_{dc}/u_{rel,0} \quad (3)$$

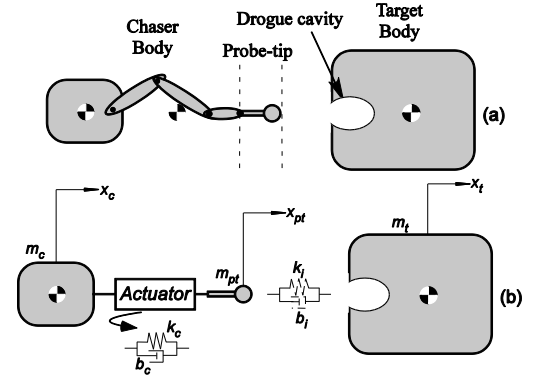


Figure 2. Model of the Chaser spacecraft with probe impacting on the drogue-equipped Target spacecraft.

III. IMPEDANCE CONTROLLER DESIGN

In this section, an impedance filter for the appropriate control of the probe-tip is introduced aiming in a desired impact behavior. The equations of motion of the system shown in Figure 2, are the following:

$$m_c \ddot{x}_c = -F_c \quad (4)$$

$$m_{pt} \ddot{x}_{pt} = F_c - F_i \quad (5)$$

$$m_t \ddot{x}_t = F_i \quad (6)$$

where F_c is the controlled force applied on the probe-tip and F_i is the impact force between the probe-tip and drogue.

To achieve a desired impact behavior, the interaction force can be controlled by an impedance controller with appropriate parameters. The impedance filter is selected as:

$$m_f (\ddot{x}_{pt} - \ddot{x}_c) + b_f (\dot{x}_{pt} - \dot{x}_c) + k_f (x_{pt} - x_c) = -F_i \quad (7)$$

where m_f , b_f , k_f are the mass, spring and damper impedance parameters to be determined. The selection of these is of paramount importance as they affect the success of docking directly. Using (4)-(7), the applied actuator force F_c required to achieve the desired impedance behavior of (7), is

$$F_c = F_i \left(\frac{((m_f/m_{pt} - 1)\mu_{c,ef})/m_f}{\mu_{c,ef} b_f (\dot{x}_c - \dot{x}_{pt})/m_f} + \mu_{c,ef} k_f (x_c - x_{pt})/m_f \right) \quad (8)$$

where $\mu_{c,ef}$ is the effective mass of the Chaser,

$$\mu_{c,ef} = m_{pt} m_c / (m_{pt} + m_c) \quad (9)$$

Selecting the m_f equal to m_{pt} , F_c does not depend on F_i and as a result a F/T sensor is not required. Then, the controlled force F_c reduces to:

$$F_c = k_d (\dot{x}_c - \dot{x}_{pt}) + k_p (x_c - x_{pt}) \quad (10)$$

where k_p , k_d are controller gains given by,

$$k_d = \mu_{c,ef} b_f / m_f, \quad k_p = \mu_{c,ef} k_f / m_f \quad (11)$$

IV. PASSIVE SYSTEM

For a better understanding of the system under observation, the behavior of the actuator is represented by a spring-

damper system, see Figure 2b, with spring stiffness k_c and damper coefficient equal to b_c . The correspondence of the passive system to the active one can be seen by setting:

$$k_c = k_p \text{ and } b_c = k_d \quad (12)$$

Once the desired behavior is established using passive system experiments and analysis, (11) and (12) allow the selection of the impedance filter parameters, for the robotic manipulator control.

Focusing on the passive spring-damper system, during docking and after the first impact between the probe-tip and the drogue, the former tends to bounce back, as the large mass of the Target base is initially unaffected by the impact with the small probe-tip mass. The Chaser base, also of large mass compared to the probe, pushes the probe-tip through the spring, forcing it to small amplitude and high frequency chatter, not affecting the Chaser base motion. To reduce this chatter, a mechanical spring pretension is introduced which results in a nonlinear spring behavior. This can be approximated by an equivalent spring, given by a describing function equivalent as

$$k_c = k_{cp} + 4k_{cp}p/\pi A \quad (13)$$

where k_c is the equivalent spring without pretension, k_{cp} is the pre-tensed spring, p is the pretension length and A is the amplitude achieved during chattering.

Impact time. This system has two natural frequencies. The high natural frequency corresponds to the fast oscillation between the low-mass probe-tip and the drogue cavity inner wall, while the low natural frequency corresponds to the slow relative motion between the two spacecraft bases; this is the one responsible for the total impact time.

The compression and restitution phases of the impact can be approximated as part of a harmonic motion; it can be described as the half-period of a sinusoidal motion with period T_{imp} . In fact, for impact durations of less than 1 s, this approach yields very good results. Thus, the duration of the impact is,

$$t_{imp} = T_{imp}/2 = \pi/\omega_d \quad (14)$$

where ω_d is the damped frequency given by,

$$\omega_d = \sqrt{1 - \zeta^2} \omega_0 \quad (15)$$

where ω_0 is the slow natural frequency,

$$\omega_0 = \sqrt{k/\mu} \quad (16)$$

and ζ is the damping ratio given by,

$$\zeta = b/2\sqrt{k\mu} \quad (17)$$

The k is the equivalent spring constant for springs in series,

$$k = k_c k_i / (k_c + k_i) \quad (18)$$

and b is the equivalent damper for dampers in series,

$$b = b_c b_i / (b_c + b_i) \quad (19)$$

where, b_c is found assuming critical damping for the tip as,

$$b_c = 2\sqrt{m_{pt}k_c} \quad (20)$$

The contact between two metallic bodies is lightly damped. Then, the value of the ‘‘fictitious’’ damper, b_i is taken as 1-10% of the value that results in critical damping, $b_{i,cr}$. i.e. of,

$$b_{i,cr} = 2\sqrt{\mu k_i} \quad (21)$$

The equivalent two-body system mass μ is:

$$\mu = m_c m_t / (m_c + m_t) \quad (22)$$

From (14), it can be seen that the lower the axial spring stiffness k is, the longer the total impact time t_{imp} becomes.

To study how the Chaser and Target masses affect the total impact time, for a given axial spring stiffness k_c , the masses of both Chaser and Target are varied and the term $\pi\sqrt{\mu} = t_{imp}\sqrt{1 - \zeta^2}\sqrt{k}$ is obtained as a function of these masses, see Figure 3. This figure shows that increasing either m_c or m_t results in longer total impact time t_{imp} . Thus, for a given Target spacecraft of mass m_t , a larger Chaser mass m_c results in a longer total impact time t_{imp} .

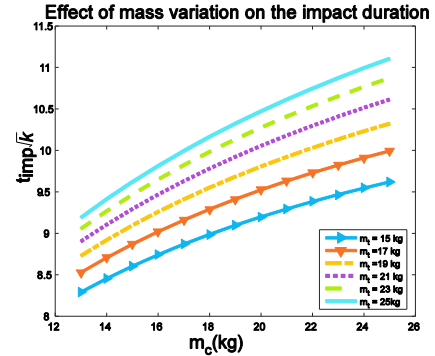


Figure 3. Effect of mass variation on impact duration.

Post-impact velocity. The impact results in a change in the relative speed between Chaser and Target. The Chaser-Target relative speed before and after the impact is,

$$u_{rel,0} = \dot{x}_{t,0} - \dot{x}_{c,0} \quad (23)$$

$$u_{rel,f} = \dot{x}_{t,f} - \dot{x}_{c,f}$$

respectively, where $\dot{x}_{c,0}, \dot{x}_{t,0}$ are the initial velocities (just before the impact) and $\dot{x}_{c,f}, \dot{x}_{t,f}$ are the final velocities (at separation, right after the impact) of the Chaser and Target spacecraft respectively.

Then, the exiting time t_{ex} can be obtained by

$$t_{ex} = d_{dc}/u_{rel,f} \quad (24)$$

It is observed that the lower $u_{rel,f}$ is, the longer t_{ex} becomes.

Thus, summing up the results for all three phases of docking, to increase the total time t_{tot} , so that (2) holds, the following are required:

- (i) Low approaching velocity $u_{rel,0}$.
- (ii) Low axial spring stiffness k_c at the probe.
- (iii) High Chaser and Target spacecraft masses m_c , and m_t . For a given m_t , then high m_c is required.

The above requirements can be used as design guidelines, both in the Chaser spacecraft design, regarding its mass m_c , the end-effector axial stiffness k_c , and the impact materials, in mission planning, regarding the approach/impact velocity $u_{rel,0}$. More importantly, they can be used as guidelines in setting the Chaser manipulator impedance control parameters.

V. EXPERIMENTAL RESULTS AND VALIDATION

To verify the theoretical estimation of the docking time and estimate the impedance parameters of the impedance controller, a set of experiments was run at the 2D Space Robotics Emulator of the CSL at the NTUA. The emulator

consists of a flat granite table on which robots on air-bearings can move, practically without friction. Since the robots are completely autonomous, they move as they would move in zero-g, although in planar, 2D motions.

For the docking experiments, two robots were used: the Chaser spacecraft, which is active, and the Target spacecraft, which is passive. The Chaser is equipped with three pairs of thrusters (each providing a force of 1.2 N in on-off, in PWM, or in PWP mode), and a reaction wheel. For localization, both robots are equipped with sets of LEDs, used by a PhaseSpace motion capture system with accuracy less than 0.5 mm, see also [18]. The Chaser is equipped with a probe, at the base of which a Force/Torque (F/T) sensor is installed in order to measure the experimental impact time, while the Target is equipped with the corresponding drogue, see also [4]. Figure 4 shows the two spacecraft robots during a docking experiment.

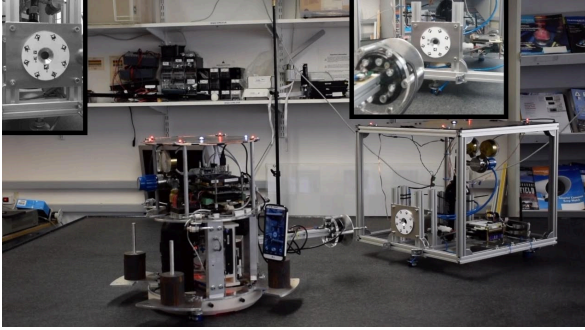


Figure 4. The probe-equipped Chaser spacecraft robot (left) approaching the drogue-equipped Target spacecraft robot, during a docking experiment at the CSL 2D Space Emulator facility. The inserts show Chaser video images.

The Chaser via a PD controller moves along the straight line that the two robot CMs form. Just prior to the entrance of the probe in the drogue, the Chaser thrusters are turned off, leaving the Chaser and probe to move freely at constant velocity, until the impact in the far end of the drogue cavity on the Target occurs. Turning off active control prior to impact, is common practice in autonomous docking, as it eliminates stresses that may occur due to the action of spacecraft attitude/position control systems.

The impact sets the Target into motion and the relative speed between Chaser and Target becomes such that the probe exits the drogue cavity again. As, ideally, both robot CMs, the probe-tip and the impact point on the drogue cavity lay on a straight line, all motions lay also on that line.

To find the appropriate values of the pre-tensed spring k_{cp} and as a result of the k_c , as well as to verify the available docking time estimated, various experiments and simulations were executed. First, the masses of the Chaser and Target were set at $m_c = 23$ kg and $m_t = 15.1$ kg respectively. The probe-tip mass is $m_{pt} = 0.003$ kg in all experiments. To study the effect of k_c and $u_{rel,0}$, on the t_{imp} , nine experiments were run in which both k_c and $u_{rel,0}$ took low, medium and high values. Furthermore, to study the effect of Chaser and Target mass on the docking time, experiments were run, not only with the initial masses, but also with lower Chaser mass (with Target mass as in the initial set), and with higher Target mass (with Chaser mass as in the initial set), see also Table 1 to Table 3. With the results of these experiments, the two controller gains k_p and k_d were calculated using (12) and thanks to $m_f = m_{pt}$ the impedance parameters result as:

$$b_f = k_d m_f / \mu_{c,ef}, k_f = k_p m_f / \mu_{c,ef} \quad (25)$$

All parameter sets that were used can be seen in Table 1 to Table 3. For all experiments and simulations, the desired docking time (see also Eq. (2)) was $t_d = 1.5$ s. This time is related with the time that an actual probe like the one depicted in Figure 1 would need to deploy.

To obtain the required velocities and time durations, first the pre-impact velocity of the Chaser (which is the initial relative velocity $u_{rel,0}$, since the Target is initially stationary) is obtained by the PhaseSpace MoCap system. In Figure 5 the pose of the Chaser is shown, for an experiment with $k_{cp} = 130$ N/m, $m_c = 23$ kg and $m_t = 15.1$ kg.

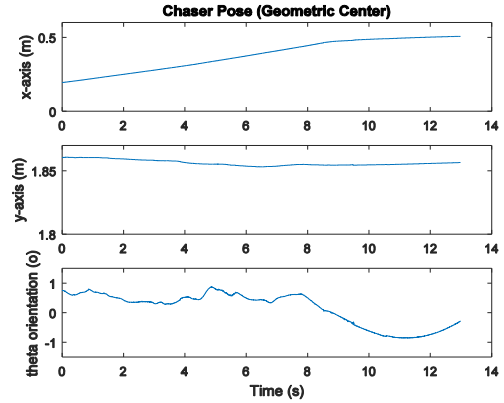


Figure 5. Chaser pose history during the experiment with $k_{cp}=130$ N/m, $m_c = 23$ kg, $m_t = 15.1$ kg and $m_{pt} = 0.003$ kg.

Note that the Chaser motion in the y-axis and its rotation around the z-axis are not constant due to external disturbances and the time that the PD controller shut down the robot's thrusters. However, the change of the motion in the y-axis before and after the impact is negligible, confirming the central impact hypothesis. Figure 5 shows that the x-axis motion consists of two straight lines with constant inclinations, thus constant initial ($\dot{x}_{c,0}$) and final ($\dot{x}_{c,f}$) velocities can be obtained. Moreover, it can be seen that the Chaser keeps on moving forward even after the impact (occurring at around 8.4 s), but with lower post-impact velocity. In this figure, the computed Chaser velocities are $\dot{x}_{c,0} = 0.038$ m/s and $\dot{x}_{c,f} = 0.00868$ m/s.

The experimental duration of the impact t_{imp} is measured by use of the F/T sensor data. As seen in Figure 6, the F/T sensor measures the impact force along its z-axis, with small forces in magnitude measured along the other two axes for the reasons mentioned above. The measured t_{imp} for this experiment was found to be 0.79 s. Finally, the experimental total time t_{tot} is obtained by the measurement of the robots relative velocity, the impact and by Eq. (1).

The experimental impact time t_{imp} can, then, be compared to the ones that are given by Eq. (14). As can be seen in Table 2 the error between the theoretical and experimental time of contact is around 10% which is assumed to be reasonable for responses involving impact modeling.

Since we have obtained the system docking response for the tried spring damper sets, we then compute the corresponding impedance gains and parameters, and simulate the controlled system response to find the t_{imp} and t_{tot} , and compare these to the ones obtained experimentally. To this end, a series of simulations using MATLAB/Simulink were

run. The Target has been modeled as a mass with cavity, while the Chaser as an impedance-controlled two-mass system. The contact forces between the bodies under impact were calculated using the KV model [9]. The initial relative velocity is constant since the Target is initially stationary, and is the same as the one used in the experiments. When the systems come into contact, a force is developed which pushes away the masses under impact and at the same time the impedance controller exerts a specific force as prescribed by the impedance filter. During the simulations, the total time during which the probe stays inside the drogue cavity, and the final relative velocity, are calculated and compared with the experimental ones. Upon this comparison, impedance parameters k_f and b_f can be obtained, that correspond to successful docking through the use of (25).

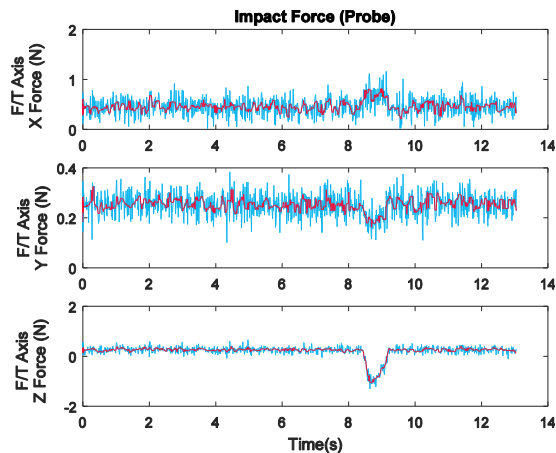


Figure 6. Probe F/T sensor reading during the experiment with $k_{cp}=130\text{N/m}$, $m_c = 23 \text{ kg}$, $m_t = 15.1 \text{ kg}$ and $m_{pt} = 0.003 \text{ kg}$.

The spring with $k_{cp} = 130 \text{ N/m}$ with pretension of 2 mm yields the same results as with one of $k_c = 147 \text{ N/m}$ without the existence of the pretension given by (13). This spring's stiffness gives an impedance parameter of $k_f = 147.0192 \text{ N/m}$ and impedance damping ration of $b_f = 1.32833 \text{ Ns/m}$. Using these impedance parameters we can observe in Figure 7d that the control force applied to the tip is reasonable in magnitude and thanks to the derivative gain, it settles down just after the impact force is zeroed. The impact force and the controller force are almost identical due to the small mass of the probe tip. For the parameters mentioned above and for the probe tip mass of $m_{pt} = 0.003 \text{ kg}$, the impact time is 0.8 s and the total time 1.36 s, both of them close to the experimental results. Moreover, from Figure 6 and Figure 7a, we can observe that the experimental and simulated impact force has the same peak in absolute value. In the case that m_{pt} is bigger e.g. $m_{pt} = 3\text{kg}$, then the controller force and the impact force as depicted in Figure 7b-c are not the same in magnitude and duration. Nevertheless, even in that case, the controller force settles down just after the last impact occurs. In the case that the impedance gains are selected arbitrary, the impact force is smaller in duration from the experimental one.

The experimental post-impact relative velocities and those derived from the simulation using the impedance controller by making the appropriate choice of its parameters are shown in Table 1. As can be seen, the per cent error is 10% apart from some values which can be explained to external disturbances. Some values of these errors can be explained as the experimental results showed a small, but

non-negligible, post impact motion of both Chaser and Target in the y-axis (i.e. perpendicular to the 1D motion axis), indicating non-negligible energy loss also in that direction, and thus slower motion in the main motion direction. The experimental and estimated impact duration t_{imp} is shown in Table 2. As can be seen, the per cent error of the estimation is even lower than the errors in the estimated $u_{rel,f}$ due to the fact that the impact time is related mostly to the materials and the masses of the systems under contact.

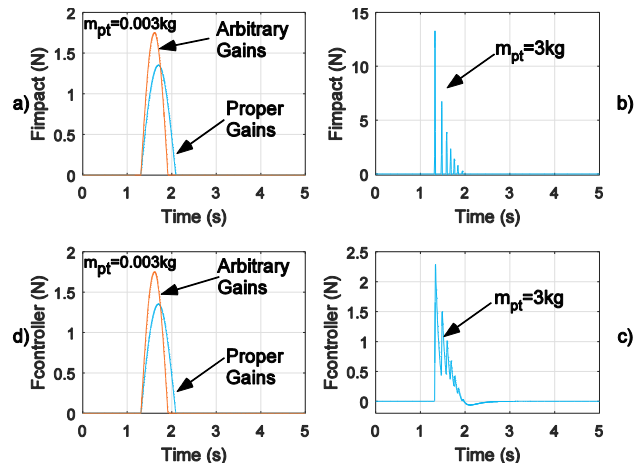


Figure 7. (a) Impact force for $m_{pt} = 0.003\text{kg}$, (b) Impact force for $m_{pt} = 3\text{kg}$ (c). Impedance controller force for $m_{pt} = 3\text{kg}$ (d). Impedance controller force for $m_{pt} = 0.003\text{kg}$

Table 1. Experimental and estimated Chaser-Target post-impact relative velocities $u_{rel,f}$.

Experiments (for all: $m_{pt} = 0.003 \text{ kg}$)				$u_{rel,f}$ (sim.) (mm/s)	$u_{rel,f}$ (exper.) (mm/s)	$e_{u_{rel}}$ (%)
m_c, m_t (kg)	k_{cp} (N/m)	k_c (N/m)	$u_{rel,0}$ (mm/s)			
23, 15.1	(A) 130	168	(1) 19	17.96	16.7	7.5
		157	(2) 25	23.63	21.9	7.9
		147	(3) 38	35.92	34	5.6
	(B) 220	268	(1) 15	14.18	11.7	21.2
		262	(2) 18	17.02	14.2	19.9
		242	(3) 38	35.92	33	8.8
	(C) 270	335	(1) 16	15.12	13.3	13.7
		398	(2) 25	23.63	19.9	18.7
		298	(3) 29	27.41	26.7	2.7
19.2, 15.1	(D) 220	253	22	20.75	16.7	24.3
23, 17.15	(E) 220	260	18	17.05	15.9	7.2

As can be seen from the five cases in Table 2 with $k_c \approx 240\text{-}268 \text{ N/m}$, (corresponding to the five cases with $k_{cp} = 220 \text{ N/m}$ in Table 1, i.e. cases B, D and E), the simulated impact time t_{imp} drops from about 0.58 s to 0.55 s, when the Chaser mass drops from 23 kg to 19.2 kg (with the Target mass kept at 15.1 kg). Moreover, the experimental t_{imp} drops from about 0.63s to 0.615s, for the same Chaser mass change. Note also that the experimental t_{imp} rises to 0.66 s when the Target mass is raised to 17.15 kg (with the Chaser mass kept at 23 kg).

The experimental and estimated total available docking time t_{tot} is seen in Table 3. Again the per cent errors are around 10%. As seen in the cases with the same initial relative velocity, i.e. the same impact velocity, the lower the axial spring stiffness is, the longer the experimental t_{tot} becomes, in accordance with the developed theory. This can be observed by comparing Case A-2 to Case C-2, both with

$u_{rel,0} = 25$ mm/s. By lowering k_c from 270 N/m (Case C-2) to 130 N/m (Case A-2), the total available docking time becomes longer by 218 ms (i.e. 14.3 %). Similar results are obtained by comparing other cases with similar $u_{rel,0}$, such as Case A-1 to Case B-2, Case A-3 to Case B-3 and Case B-1 to Case C-1 in Table 3.

Furthermore, for the same axial spring stiffness k_{cp} and the same Chaser and Target masses, the lower the impact velocity is, the longer the t_{tot} results. For example, for the three experiments of Case A, with $k_{cp} = 130$ N/m, as the initial relative (i.e impact) velocity drops from 38 mm/s to 25 mm/s (34.2 % drop), and then to 19 mm/s (further 24 % drop), the experimental t_{tot} rises from 1.363 s to 1.739 s (27.6 % rise) and then to 2.249 s (a further 29.3 % rise). These results confirm the first two theoretical guidelines, proposed at the end of Section IV.

Table 2. Experimental and estimated impact duration.

Experiments (for all: $m_{pt} = 0.003$ kg)			t_{imp} (theor.) (s)	t_{imp} (exper.) (s)	t_{imp} (sim.) (s)	$\epsilon_{th,exp}$ (%)	$\epsilon_{sim-exp}$ (%)
$m_c,$ m_t (kg)	k_c (N/m)	$u_{rel,0}$ (mm/s)					
23, 15.1	168	(1) 19	0.75	0.77	0.75	2.18	3.25
	157	(2) 25	0.77	0.73	0.78	5.77	6.3
	147	(3) 38	0.79	0.79	0.8	0.55	1.27
	268	(1) 15	0.54	0.63	0.57	13.6	10
	262	(2) 18	0.56	0.635	0.58	12.1	8.77
	242	(3) 38	0.6	0.624	0.6	3.76	3.2
	335	(1) 16	0.49	0.56	0.49	12.7	11.9
	398	(2) 25	0.52	0.6	0.52	13.7	12.7
19.2, 15.1	253	22	0.55	0.615	0.55	10.9	10.7
23, 17.15	260	18	0.58	0.66	0.58	11.6	11.5

Table 3. Experimental and estimated available total docking time.

Experiments (for all: $m_{pt} = 0.003$ kg)			t_{tot} (estim.) (s)	t_{tot} (exper.) (s)	$\epsilon_{t_{tot}}$ (%)
m_c, m_t (kg)	k_{cp} (N/m)	$u_{rel,0}$ (mm/s)			
23, 15.1	(A) 130	(1) 19	1.87	2.249	16.79
		(2) 25	1.63	1.739	6.11
		(3) 38	1.36	1.363	0.02
	(B) 220	(1) 15	1.99	2.625	24
		(2) 18	1.77	2.02	12.5
		(3) 38	1.17	1.225	4.72
	(C) 270	(1) 16	1.83	2.162	15.31
		(2) 25	1.38	1.521	9.28
		(3) 29	1.27	1.382	8.39
19.2, 15.1	(D) 220	22	1.52	1.64	7.15
23, 17.15	(E) 220	18	1.77	1.94	8.66

Finally, by comparing experimental Case D to Case B-2, it can be observed that, lowering the Chaser mass m_c results in smaller total time available for docking (t_{tot}), while by comparing Case E to Case B-2, it can be observed that higher Target mass m_t , results in longer t_{tot} . Thus the third theoretical guideline proposed in Section IV, is also confirmed.

Having assumed that the required docking time t_d is 1.5 s, (2) and Table 3 are used to determine which condition combinations lead to successful docking both analytically, by using the right impedance parameters, and experimentally. As can be observed, both experiments and simulations with the controlled system classify the cases similarly, i.e. as successful or unsuccessful.

VI. CONCLUSION

An important phase in OOS tasks is autonomous robotic docking; this is subject to a number of parameters and conditions. In this paper, docking of a robotic Chaser to a Target spacecraft employing an impedance-controlled manipulator was studied. The relation of the impedance gains and as a result the impedance parameters to their mechanical counterparts was established. The time that the end-effector remains in the drogue was derived analytically to display the effect of system parameters and conditions affecting it, and to yield design guidelines. Experiments performed on a planar zero-g emulator facility showed satisfactory agreement between the experimental and analytical results using a single-axis hypothesis to draw conclusions of the aforementioned relation.

REFERENCES

- [1] Oda, M., Kibe, K., and Yamagata, F. (1996) "ETS-VII, space robot in-orbit experiment satellite," *Int. Conf. on Robotics and Automation (ICRA'96)*, Minneapolis, USA, April 1996, pp. 739-744.
- [2] <http://archive.darpa.mil/orbitalexpress/index.html>
- [3] http://ssco.gsfc.nasa.gov/rm_refueling_task.html
- [4] Medina, A., et al., "Towards a standardized grasping and refueling on-orbit servicing for GEO spacecraft", *66th International Astronautical Congress 2015 (IAC '15)*, October 2015, Jerusalem, Israel.
- [5] Fehse, W. (2003). *Automated Rendezvous and Docking of Spacecraft*, Cambridge University Press, ISBN 9780521089869.
- [6] Dimitrov, D. N., and Yoshida, K. "Momentum distribution in a space manipulator for facilitating the post-impact control," *Int. Conf. on Intelligent Robots and Systems (IROS '04)*, Japan, pp. 3345-3350.
- [7] Flores-Abad, A., Pham, K., and Ma, O. "Control of a Space Robot for Capturing a Tumbling Object," *Int. Symp. on Artificial Intelligence, Robotics & Automation in Space*, (i-SAIRAS 2012). Turin, Italy.
- [8] Gilardi, G. and Sharf, I., "Literature Survey of Contact Dynamics Modelling," *Mech. & Machine Th.*, 37(10), 2002, pp. 1213-1239.
- [9] Stronge, W. J., *Impact Mechanics*, Cambridge Univ. Press, 2000.
- [10] Zebenay, M., T. Boge, D. Choukroun, (2014), "Modeling, Stability Analysis, and Testing of a Hybrid Docking Simulator," *Acta Astronautica*, 00, pp. 1-30.
- [11] Uyama, N., Nakanishi, H., Nagaoka, K., and Yoshida, K., "Impedance-Based Contact Control of a Free-Flying Space Robot with a Compliant Wrist for Non-Cooperative Satellite Capture," *IEEE/RSJ Int. Conf. on Intelligent Robots and Systems (IROS '12)*, Vilamoura, Algarve, Portugal, October 2014, pp. 4477-4482.
- [12] Yoshida, K., and Nakanishi, H. "Impedance Matching in Capturing a Satellite by a Space Robot," *Int. Conf. on Intelligent Robots and Systems (IROS '03)*, Las Vegas, Nevada, pp. 3059-3064.
- [13] Moosavian, S. Ali A. and Papadopoulos, E. (1998) "Multiple Impedance Control for Object Manipulation," *Int. Conf. on Intelligent Robots and Systems (IROS '98)*, Victoria, BC, Canada, October 1998.
- [14] N. Hogan, "Impedance Control: an approach to manipulation- A three part paper," *ASME Journal of Dynamic Systems, Measurement, and Control*, vol. 107, March 1985, pp. 1-24.
- [15] Moosavian, S. Ali A. and Papadopoulos, E. (2010) "Cooperative object manipulation with contact impact using multiple impedance control" *Int. Journal of Control, Automation, and Systems*, 8 (2), pp. 314-327.
- [16] Van Vliet, J., Sharf, I., and Ma O, (2003) "Experimental Validation of Contact Dynamics Simulation of Constrained Robotic Tasks", *International Journal of Robotics and Research* 19(12):1203-1217
- [17] Mitros, Z., Paraskevas, I.S. and Papadopoulos, E. G., "On Robotic Impact Docking for On Orbit Servicing", *Proc. 24th IEEE Mediterranean Conference on Control and Automation*, June 21-24, 2016, Athens, Greece, pp. 1120-1125.
- [18] Machairas, K., Andreou, S., Paraskevas, I. and Papadopoulos, E., "Extending the NTUA Space Robot Emulator for Validating Complex On-Orbit Servicing Tasks," *12th Symposium on Advanced Space Technologies in Robotics and Automation, (ASTRA '13)*, ESA, ESTEC, Noordwijk, The Netherlands, May 15-17, 2013.